PHYSICAL REVIEW E VOLUME 58, NUMBER 4 OCTOBER 1998

Phase diagram for avalanche stratification of granular media

J. P. Koeppe, M. Enz, and J. Kakalios
School of Physics and Astronomy, The University of Minnesota, Minneapolis, Minnesota 55455
(Received 25 August 1997)

When a binary mixture of granular materials is poured into a quasi-two-dimensional Hele-Shaw cell, alternating stratified layers of large and small particles are formed along the top surface. This effect is studied as the plate separation of the cell and the flow rate at which the granular mixture is poured are systematically varied. A nontrivial ''phase diagram'' is found, with pairing of the stratification layers occurring for a finite range of plate separation and flow rate values. Numerical simulations based upon a model involving periodic avalanching of a metastable wedge of granular material above the critical angle of repose reproduce both the observed stratification pattern and the flow rate dependence. [S1063-651X(98)51510-3]

PACS number(s): 46.10.+z, 47.27.Te, 64.60.Lx, 64.75.+g

Binary mixtures of powders or grains can separate by particle property when poured into a vertical Hele-Shaw cell [1–3]. This phenomenon, termed ''avalanche stratification,'' where the large and small materials separate into alternating layers, occurs when an initially homogeneous mixture of two different granular materials is poured between two vertical plates held a narrow distance apart. An elucidation of the mechanisms responsible for avalanche stratification may be important for understanding many geological formations [1,4–7], as well as industrial processes that require that mixtures poured from a hopper remain homogeneous [8]. Models by Makse, Cizeau, and Stanley [9], Boutreaux and de Gennes [10], and Grassellli and Herrmann [11] can successfully account for the observed avalanche segregation and stratification patterns for a given Hele-Shaw cell. However, these models are strictly two-dimensional, while experiments find that the stratification pattern is sensitive to the separation of the vertical plates [3]. In this Rapid Communication we report experimental studies of avalanche stratification as the plate separation and flow rate of the poured mixture are systematically varied, which yields a nontrivial phase diagram of the stratification effect.

The experimental setup [Fig. 1(a)] consists of two vertical Plexiglas sheets 6 mm thick of area 10.5×8 in. mounted parallel to each other on a horizontal base plate. One sheet is fixed to the base plate, while the other sheet is attached at one end to the fixed plate. By employing spacers that extend the full height of the vertical sheets (so that one end remains closed) the separation between the plates can be varied from 3 to 24 mm. A 50/50 mixture by mass of black sand (roughly spherical with an average diameter of 0.4 mm and a density of 1.5 mg/mm^3) and white sugar (roughly cylindrical, with an average long axis of 0.8 mm and a density of 0.5 mg/mm^3) is poured against the closed edge of this Hele-Shaw cell using a titrating bulb with a rotating stopcock. The granular mixture has an average density of 1.0 mg/mm^3 and is premixed by stirring prior to pouring. Sampling of the granular mixture exiting the flow bulb onto a flat surface confirms that the granular material does not undergo segregation either exiting the bulb or while falling into the cell, though possible segregation prior to discharge may still remain an issue. The stratification pattern in Fig. 1(b) was obtained for a plate separation d of 4 mm and a flow rate f of 0.78 g/sec, when the sand/sugar mixture is poured against the closed edge of the cell (similar patterns are found when the mixture is poured in the center of the cell [3]). The flow rates can be varied from 0.3 to 3.7 g/sec. The static angle of repose of the sand is 37.3° and of the sugar is 40°, while the angle of repose of sand on sugar is 40.3° and of sugar on sand is 39.8°. Digital images of the stratification pattern [Fig. 1(b)] are taken with a monochrome charge-coupled-device camera (Cohu 4910) in conjunction with a Scion LG-3 frame grabber and a Power Macintosh 7100/80. Data image analysis is performed using the public domain program Image from the National Institute of Health.

In order to quantify the intensity and wavelength of the stratification effect, digital images of the banding pattern

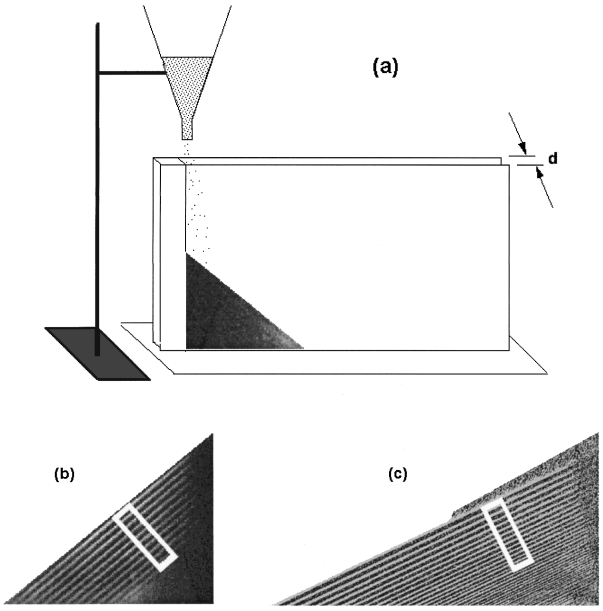

FIG. 1. Sketch of the avalanche stratification apparatus (a) wherein a mixture of two different granular materials is poured against the closed edge of a Hele-Shaw cell. (b) A digital image of the resulting stratification pattern for a 50/50 mixture (by mass) of sand and sugar. The flow rate was 0.78 g/sec and the plate separation was 4 mm. (c) The resulting stratification pattern for a numerical simulation of a physical model of poured two-dimensional granular mixtures, as described in the text.

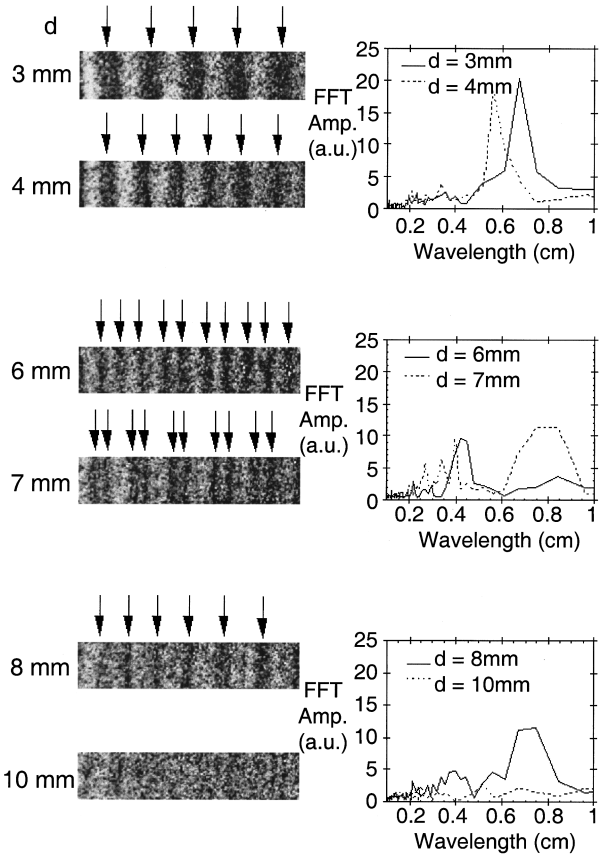

FIG. 2. Digital images (a) of the stratification banding pattern near the top of the pile [indicated by the white box in Fig. 1(b)] and plots of the corresponding Fourier amplitude against wavelength (b) for the sand/sugar mixture of Fig. 1 as the plate separation of the Hele-Shaw cell is varied from 3 to 10 mm (flow rate 0.78 g/sec). The arrows in (a) indicate the layers of sand (dyed dark).

near the top of the sandpile are Fourier analyzed. The digital image in the white box in Fig. 1(b) is converted into a plot of pixel intensity against position. Since the sand is black and the sugar is white, a high pixel value corresponds to a large concentration of sand next to the transparent vertical plate in the Hele-Shaw cell, while a low pixel value corresponds to a high concentration of sugar and an intermediate pixel value reflects a mixture of the two. The resulting plot of varying pixel value against position (depth into the sandpile) is then Fourier transformed to yield the structure function of the stratification pattern. While the structure function is the square of the Fourier amplitude and is typically plotted against a wave vector, for simplicity the fast Fourier transform (FFT) amplitude is plotted against a wavelength in Fig. 2. As shown in Fig. 2, the characteristic wavelength and the degree of stratification, as reflected in the position and amplitude of the peak of the FFT amplitude, respectively, are sensitive to the plate separation d of the Hele-Shaw cell. For a flow rate of 0.78 g/sec, as d is increased from 3 to 10 mm, both the wavelength and FFT amplitude decrease. Moreover, for an intermediate plate separation of $\sim$7 mm, clear ''pairing'' of adjacent stratification layers of sand is evident, confirmed by the second peak in the corresponding FFT amplitude in Fig. 2(b). For this granular system, by $d=10$ mm there is little indication of stratification.

The sensitivity of the stratification pattern to varying the

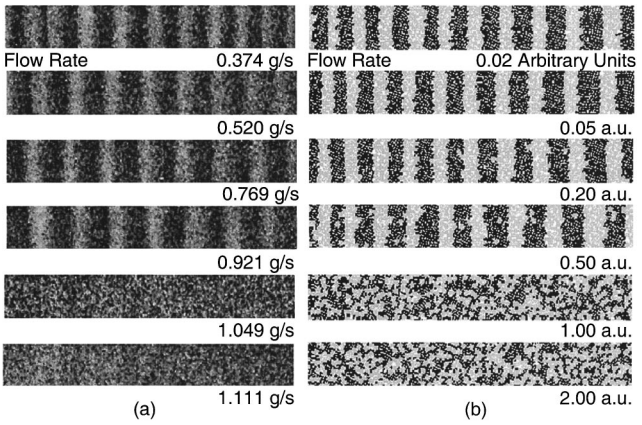

FIG. 3. (a) Digital images of the stratification pattern near the top of the pile [indicated by the white box in Fig. 1(b)] for six separate runs as the flow rate is increased. (b) Computer simulations as in Fig. (1c), using the physical model described in the text, as the rate (arb. units) at which granular material was added to the top right-hand edge is increased, relative to the timing of relaxation of the metastable heap at the top of the pile.

flow rate f at which the granular mixture is poured into the Hele-Shaw cell, for a fixed plate separation, has also been investigated. The resulting banding patterns are shown in Fig. 3(a). Fourier analysis of the banding patterns finds that the degree of stratification exhibits a sharp decrease at a critical flow rate of $f_c \sim 1.0$ g/sec. For flows greater than this critical rate (which depends on the plate separation) the stratification pattern abruptly disappears. In contrast to the plate separation dependence, the wavelength of the stratification pattern is roughly insensitive to the flow rate, though the rapid loss of stratification above f_c limits the range for which this parameter can be investigated.

These experiments have been repeated for a series of plate separations and flow rates. The results are summarized in Fig. 4, which is a ''phase diagram,'' indicating whether or

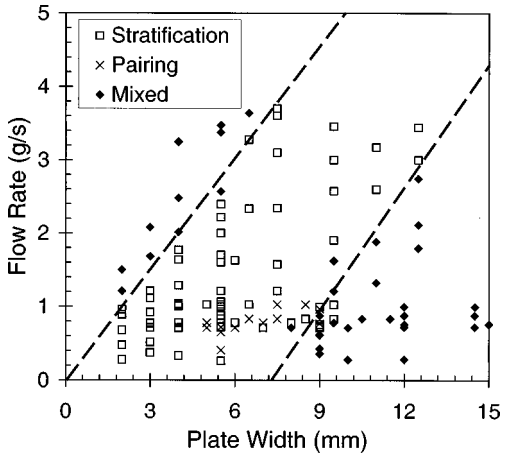

FIG. 4. ''Phase diagram'' for the avalanche stratification effect for a 50/50 mixture of sand and sugar. The open squares indicate those plate separations and flow rates for which stratification is observed, while the closed diamonds denote that no layering was found (the dashed lines are guides to the eye). The cross symbols represent the plate separation and flow rates for which pairing of the stratified bands occurred.

not stratification is observed for a given flow rate and plate separation. The open squares indicate that stratification occurred [defined as a Fourier peak amplitude greater than 6, as in Fig. 2(b)], while the closed diamonds represent those flow rates and plate separations for which no layering was found. The crosses denote those f and d values for which pairing of the stratification layers was observed. The data in Fig. 4 have been reproduced for many separate measurement runs over a period of several months. Qualitatively similar results are found for avalanche stratification of a mixture of glass beads and couscous. The results of Fig. 4 demonstrate that the stratification effect occurs only for a finite range of flow rates and plate separations.

Previous models for stratification in a Hele-Shaw cell required that the larger and more faceted granular material have a larger angle of repose compared to the smaller and smoother material, which leads to separation of the two species as they roll down the free surface, with the smaller material becoming fixed in irregularities of the granular surface [2,9–11]. Numerical simulations of avalanche stratification by Makse and co-workers [9,11] are able to faithfully recreate an observed avalanche stratification pattern for a given flow rate as in Fig. 1(b). However, we have observed stratification layers for a mixture of large and small glass beads of the same density, for which the measured angle of repose of these beads differ by only 0.1°, which cannot be accounted for by this model.

We consequently consider a model for the stratification pattern involving periodic avalanching of granular material between the maximum and critical angles of repose [12–15]. As granular material is poured into the Hele-Shaw cell, a quasi-two-dimensional sandpile forms at the angle of repose of the mixture. Inelastic collisions cause some of the grains rolling down the top surface to come to rest and form a metastable heap [16]. When the maximum angle of stability is reached, the material in the heap avalanches down the top surface, returning the top of the pile to the critical angle of repose. The strong velocity gradient normal to the surface of the flowing pile leads to shear dilation [17], which in turn enables separation or sieving of the smaller or denser granular material to fall into small gaps or voids in the flowing surface beneath the larger or less dense material in the flowing layer [13–15]. In particle dynamics simulations based upon this model large and small discs are dropped at random against a vertical boundary, as in Ref. [9], and then lose a fixed fraction of their kinetic energy with every collision with other discs. When the kinetic energy is below a threshold value, and the horizontal center of mass of the disc is lower than or equal to the horizontal center of mass of the adjacent discs, the falling disc then stops moving. However, the resulting two-dimensional pile is much steeper than for experimentally observed sandpiles. Two input parameters were then added to the simulations, the maximum and critical angle of repose of the entire mixed sandpile, so that when granular material is added such that the height of the pile exceeds the maximum angle of repose, the discs contained in the wedge between the maximum and critical angles of repose are given additional energy (proportional to their gravitational potential energy at the top of the pile) and allowed to avalanche down the top surface, coming to rest using the mechanical stability criteria. As shown in Fig. 1(c) these simulations do indeed reproduce the observed stratification pattern. The flow rate can be increased by varying the rate at which discs are dropped onto the pile relative to the rate at which the metastable heap on the top can relax. Strikingly similar results are found for the computer simulations [Fig. 3(b)], with the strength of the stratification and the wavelength of the banding pattern being fairly insensitive to the flow rate until a critical f_c is reached, at which point the stratification abruptly and sharply disappears. When $f > f_c$, the ''grainfall'' along the top surface is so fast that there is no time for the development of metastable heaps at the top of the pile, while for $f < f_c$ the stratification pattern is determined by the amount of mass contained within the metastable wedge, which depends on the properties of the granular material and plate spacing d, but is independent of the rate at which the material is poured into the cell.

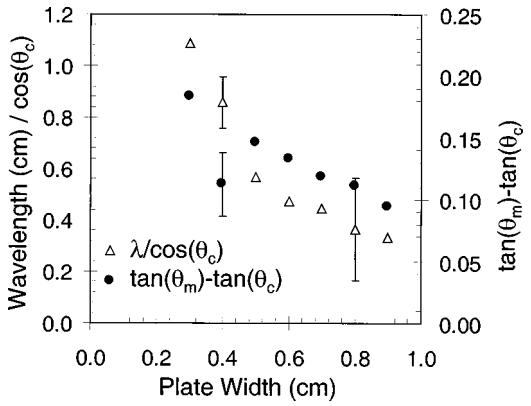

FIG. 5. Plot of the variation of the wavelength/$\cos(\theta_c)$ of the stratification pattern (open triangles) and the quantity $[\tan(\theta_m) - \tan(\theta_c)]$ (closed circles) against plate separation.

The wavelength of the stratified layers will be proportional to the mass of granular material contained in the metastable wedge prior to avalanching. The amount of mass contained in the metastable wedge is given by $(\rho_m x^2 d/2)$ $[\tan(\theta_m) - \tan(\theta_c)]$ where ρ_m is the density of the binary granular mixture and x is the distance the pile extends along the horizontal base. Following a stratification avalanche, the mass of granular material contained in the layers is given by $(\rho_1 + \rho_2)(x\lambda d)/2 \cos(\theta_c)$, where ρ_1 and ρ_2 are the densities of the separate granular species. Equating these two expressions yields $\lambda/\cos(\theta_c) = \alpha x(\rho_m/\rho_1 + \rho_2)[\tan(\theta_m) - \tan(\theta_c)]$, where the factor α $(0 < \alpha < 1)$ reflects the fact that the stratified layers do not extend the entire length of the sandpile, but rather merge into the segregated regions at the top and bottom of the pile. Grasselli and Herrmann have reported that θ_c and θ_m in a Hele-Shaw cell increases exponentially as the plate spacing is decreased [18], due to the increasing importance of transverse force chains, which span the two vertical plates and provide arching support to the granular sandpile. The variation with plate spacing of the quantities $\lambda/\cos(\theta_c)$ and $\tan(\theta_m) - \tan(\theta_c)$ are shown in Fig. 5. The data of Fig. 5 indicates that the factor $\alpha x(\rho_m/\rho_1 + \rho_2) = 3.75$ for $d \geqslant 5$ mm, which, for an average horizontal extent of the pile $x \sim 10-12$ cm, corresponds to $\alpha \sim 0.625-0.75$, which is in reasonable agreement with images of the stratification pattern as in Fig. 1(b).

The decrease in the amplitude of the stratification pattern with d may arise from sidewall interactions becoming important paradoxically at larger plate spacings. It is well known that the velocity profile of flowing granular material through a narrow inclined chute is significantly depressed in the region adjacent to each sidewall, with the relative decrease in velocity increasing for wider chutes [19]. Consequently, as the plate separation d is increased, there is an associated increase in the flow transverse to the down slope motion, as the particles follow the velocity gradients. The transverse flow tends to oppose the stratification tendency within the flowing layer, as reflected by the decrease in FFT amplitude for increasing d. Consequently the loss of stratification at large d would be a direct result of the avalanches occurring in a Hele-Shaw cell, and the model described above may still be valid for three-dimensional geological flows. A remaining mystery is the pairing of the layers [Figs. 2(a) and 2(b) for $d=6$ and 7 mm] which is reminiscent of an ''Eckhaus instability'' in driven dynamical systems [20], where changes in the pattern formation control parameter (here the plate separation d) can lead to period doubling of the spatial wavelength [21], though much more work on this point is needed.

This research was supported by the Minnesota Graduate School Grant-in-Aid Program, the Undergraduate Research Opportunity Program, and Grant No. NSF-CTS-9501437. We gratefully acknowledge experimental assistance from K. M. Hill and W. Weisman, and helpful comments from J. Gollub, P.-G. de Gennes, T. Boutreaux, H. Makse, E. G. Stanley, O. T. Valls, and H. J. Herrmann.

[1] J. C. Williams, Powder Technol. **2**, 13 (1968).

[2] Hernan A. Makse, Shlomo Havlin, Peter B. King, and H. Eugene Stanley, Nature (London) **386**, 379 (1997).

[3] J. Koeppe, M. Enz, and J. Kakalios, in *Statistical Mechanics in Physics and Biology*, edited by Denis Wirtz and Thomas C. Halsey, MRS Symposia Proceedings No. 463 (Materials Research Society, Pittsburgh, 1997), p. 319.

[4] Ian Livingstone and Andrew Warren, *Aeolian Geomorphology: An Introduction* (Addison Wesley Longman Lmt., Singapore, 1996); J. D. Collinson and D. B. Thompson, *Sedimentary Structures*, 2nd ed. (Unwin Hyman Ltd., London, 1989); J. R. L. Allen, *Sedimentary Structures: Their Character and Physical Basis* (Elsevier, Amsterdam, 1982).

[5] G. V. Middleton, *Mechanics of Sediment Movement* (Society of Economic Palontologists and Mineralogists, Providence, RI, 1984); Geo. Assoc. of Canada, special paper no. 7, 253 (1970).

[6] A. V. Jopling, J. Geophys. Res. **69**, 3403 (1964).

[7] S. G. Fryberger and C. Schenk, Sedimentology **28**, 805 (1981).

[8] R. M. Nedderman, U. Tuzun, S. B. Savage, and G. T. Houlsby, Chem. Eng. Sci. **37**, 1597 (1982).

[9] Hernan A. Makse, Pierre Cizeau, and H. Eugene Stanley, Phys. Rev. Lett. **78**, 3298 (1997); Hernan A. Makse, Phys. Rev. E **56**, 7008 (1997).

[10] T. Boutreux and P.-G. de Gennes, J. Phys. (France) **6**, 1295 (1996).

[11] Y. Grasselli and H. J. Herrmann, Granular Media (to be published); Hernan A. Makse and Hans J. Herrmann (unpublished).

[12] S. B. Savage, *Developments in Engineering Mechanics*, edited by A. P. S. Selvadurai (Elsevier, Amsterdam, 1987), p. 347; S. B. Savage and C. K. K. Lun, J. Fluid Mech. **189**, 311 (1988).

[13] K. Ridgway and R. Rupp, Powder Technol. **4**, 195 (1970).

[14] J. A. Drahun and J. Bridgwater, Powder Technol. **36**, 39 (1983).

[15] P. Y. Julien, Y. Q. Lan, and Y. Raslan, *Proceedings of the Third International Conference on Powders and Grains*, edited by Robert P. Behringer and James T. Jenkins (A. A. Balkema, Rotterdam, 1997), p. 487.

[16] The wedge described in the model arises from granular material that has stopped flowing down the top surface of the sandpile. Consequently, the static angles of repose (θ_m and θ_c) are relevant, rather than the dynamic angle of repose.

[17] R. A. Bagnold, *The Physics of Blown Sand and Desert Dunes* (Chapman and Hall, London, 1941).

[18] Y. Grasselli and H. J. Herrmann, Physica A **246**, 301 (1997).

[19] P. C. Johnson, P. Nott, and R. Jackson, J. Fluid Mech. **210**, 501 (1990); D. M. Hanes, O. Walton, V. Zakirov, G. Locurto, and R. Bucklin, *Proceedings of the Third International Conference on Powders and Grains*, edited by Robert P. Behringer and James T. Jenkins (A. A. Balkema, Rotterdam, 1997), p. 459.

[20] V. Eckhaus, *Studies in Nonlinear Stability Theory*, Springer Tracts in Natural Philososphy Vol. 6 (Springer-Verlag, Berlin, 1965).

[21] M. C. Cross and P. C. Hohenberg, Rev. Mod. Phys. **65**, 851 (1993).